PHYSOR 2002, Seoul, Korea, October 7-10, 2002

CRITICAL MASSES OF HIGHLY ENRICHED URANIUM DILUTED WITH MATRIX MATERIAL

by

Rene Sanchez, David Loaiza, and Robert Kimpland
P.O. Box 1663, MS J562
Los Alamos National Laboratory
Los Alamos, NM 87545
rsanchez@lanl.gov, dloaiza@lanl.gov, kimpland@lanl.gov

ABSTRACT

Scientist at the Los Alamos national Laboratory measured the critical masses of square-prisms of highly enriched uranium diluted in various X/^{235}U ratios with matrix material and polyethylene. The configuration cores were 22.86-cm square and 45.72-cm square and were reflected with 8.13-cm-thick and 10.16-cm--thick side polyethylene reflectors, respectively. The configurations had 10.16-cm--thick top and bottom polyethylene reflectors. For some configurations, the Rossi-α, which is an eigenvalue characteristic for a particular configuration, was measured to establish a reactivity scale based on the degree of subcriticality. Finally, the critical mass experiments are compared with values calculated with MCNP and ENDF/B-V and ENDF/B-VI cross-section data.

1. INTRODUCTION

Fissile material in waste is frequently encountered in decontamination and decommissioning activities. The radioactive waste is for the most part placed in containers or drums and stored in storage facilities throughout the Department of Energy (DOE) complex. The amount of fissile material in each drum is generally small because of criticality safety limits that have been calculated with computer transport codes such as MCNP,[1] KENO,[2] or ONEDANT.[3] To the best of our knowledge, few critical mass experiments have been performed to assure the correctness of these calculations or any calculations for systems containing fissile material (^{235}U, ^{239}Pu, ^{233}U) in contact with matrix material such as Al_2O_3, CaO, MgO, SiO_2, Gd, concrete, or Fe. The experimental

results presented in this paper establish the critical masses of highly enriched uranium (HEU) foils diluted in various X/^{235}U ratios with matrix material and polyethylene. The polyethylene is used to represent water, which is one of the elements that likely would be found in an underground radioactive waste storage facility thousands of years from now.

The diluted uranium cores were 22.86-cm square and 45.72-cm square and were reflected with 8.13-cm-thick and 10.16-cm--thick side reflectors, respectively. The top and bottom reflectors were 10.16-cm--thick. The experiments described in this paper will help validate cross--section data used in computer transport codes.

2. MATERIALS

The fissile material available consisted of approximately 39 HEU foils. The dimensions of the bare foils were approximately 22.86-cm square and 0.00762-cm thick. The foils were laminated with thin plastic sheets to reduce the amount of airborne contamination. The total thickness of the foils, including the laminating plastic sheets, was 0.02286-cm. Each foil weighed approximately 70-g and the isotopic composition was 93.23 wt % ^{235}U, 5.37 wt % ^{238}U, and 1.13 wt % ^{234}U. Table I lists the weights of each of the foils before and after lamination.

The diluent materials consisted of SiO_2 plates, high-density polyethylene inserts, 6061 aluminum plates, MgO powder, Gd foils, and Fe plates. Two types of moderating high-density polyethylene plates were used.

For the first series of experiments, the moderating high-density polyethylene plates were 39.12-cm square and 1.91-cm thick. Each polyethylene plate used in the core region had a square central recess. The dimensions of the central recess were 22.86-cm square by 0.64-cm deep. The central recess in each polyethylene plate was used to accommodate the SiO_2, or aluminum plates, or MgO powder, or polyethylene inserts. The dimensions of the SiO_2, polyethylene inserts, and aluminum plates were approximately 22.86-cm square by 0.64-cm thick.

Because the MgO is a powdery substance, the density of the MgO was determined by weighing the empty polyethylene plate and then weighing the polyethylene plate with the MgO in the recess. The density of MgO in each polyethylene plate was calculated by dividing the weight difference between the empty and filled polyethylene plate by the recess volume.

Because Gd has a very large absorption cross section at thermal energies, the Gd foils that were used in these experiments were small. Their dimensions were 5.08-cm square by 0.041-cm thick for some experiments. In order to study the effect on the critical mass and reactivity as a function of thickness of the Gd foils, other experiments were performed with thinner Gd foils. Their dimensions were 5.08-cm square by 0.02-cm-thick. The Gd foils were placed on the center of the uranium foils. These experiments were only performed with polyethylene inserts in the moderating plates.

The low--carbon steel plates, which are mostly Fe, were 22.86-cm square by 0.038-cm thick. These plates were placed on the moderating plates with polyethylene inserts followed by the HEU foils.

There were eight plates that form the top and bottom reflectors (four at the top and four at the bottom). Their dimensions were approximately 39.12-cm square by 2.54-cm thick.

For the second series of experiments, the moderating high-density polyethylene plates were of two different sizes. The ones that were used in the bottom part of the core were 66.04-cm square by 1.05-cm thick. The ones that were used in the top part of the core were 75.18-cm square by 1.05-cm thick. Both types of plates had a central recess where matrix material could be placed. The dimensions of the central recess were 45.72-cm square by 0.64-cm deep. Four plates of matrix material (SiO_2, Al, polyethylene inserts, etc.) were needed to completely fill the central recess in each moderating polyethylene plate. The experiment that was performed with this type of configuration was the 5 .08-cm square by 0.041-cm--thick Gd foils with polyethylene inserts in the moderating plates.

Table I. Weight of HEU foils before and after lamination.

Foil #	Weight before lamination	Weight after lamination
1	68 g	80 g
2	71 g	82 g
3	71 g	83 g
4	71 g	83 g
5	69 g	81 g
6	70 g	82 g
7	71 g	82 g
8	71 g	82 g
9	69 g	80 g
10	70 g	81 g
11	70 g	83 g
12	71 g	82 g
13	69 g	81 g
14	66 g	77 g
15	71 g	82 g
16	67 g	78 g
17	67 g	78 g
18	69 g	80 g
19	68 g	79 g
20	69 g	80 g
21	72 g	84 g
22	70 g	81 g
23	70 g	82 g
24	70 g	81 g
25	72 g	84 g
26	69 g	81 g
27	69.0 g	79.1 g
28	71.3 g	81.4 g
29	71.4 g	81.6 g
30	69.4 g	79.3 g
31	70.8 g	81.1 g
32	70.2 g	80.5 g
33	70.6 g	80.2 g
34	71.1 g	81.4 g
35	71.3 g	81.5 g
36	71.8 g	82.1 g
37	72.4 g	79.3 g
38	71.3 g	81.1 g
39	70.4 g	80.5 g

The Gd foils were placed on each of the four HEU foils and interspersed between moderating plates. Eight polyethylene plates (four on the top and four at the bottom) form the top and bottom reflectors. Their dimensions were 66.04-cm square by 2.54-cm thick.

3. DESCRIPTION OF EXPERIMENTS

The experiments were performed on the Planet general-purpose vertical assembly machine shown in Fig. 1. This machine consists of a hydraulic lift directly beneath a stationary aluminum platform, which lifts the bottom part of the experiment that rests on a movable platen approximately 22 cm to 30- cm. The final closure is performed with four jackscrews that are driven with a stepping motor and that move the platen the final 4.5-cm of separation very precisely. Figure 1 shows the setup for measurements of the HEU foils-SiO_2-polyethylene experiment. For the final approach to critical, typically half of the critical mass is placed on the top platform and the other half is placed on the movable platen.

As seen in Fig. 1, there is a hollow cylinder and a 10 kg weight on the top of the reflector. The weight is there to ensure that there is full compression of the stack. Because most of the experiments were not infinite reflected systems, a hollow cylinder was used to separate the 10 kg weight from the top of the reflector. This action minimizes the number of neutrons that are reflected from the 10 kg weight back into the system. Therefore, the reactivity worth of the 10 kg weight can be assumed to be zero and independent of its position on the top of the reflector.

Figure 2 shows a cross section of the experiments in their approximate final configuration. Note that the laminated HEU foils are in direct contact with the matrix material. Figure 3 shows the types of experiments that were performed with the Gd foils and Fe plates.

The starting configuration for all experiments contained less than 800 g of HEU, which is the minimum critical mass for a homogeneous water--moderated, water--reflected HEU

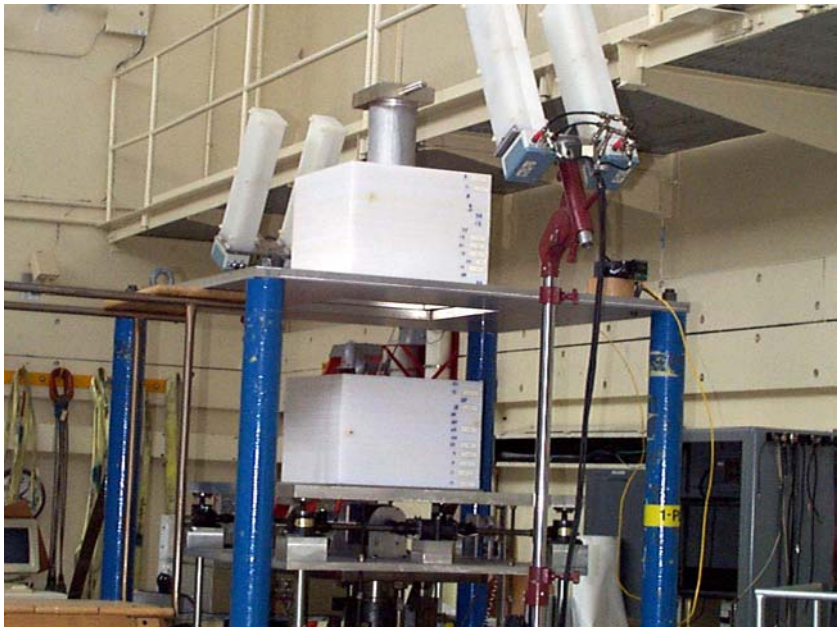

Figure 1. The HEU waste matrix experiments mounted on the Planet assembly.

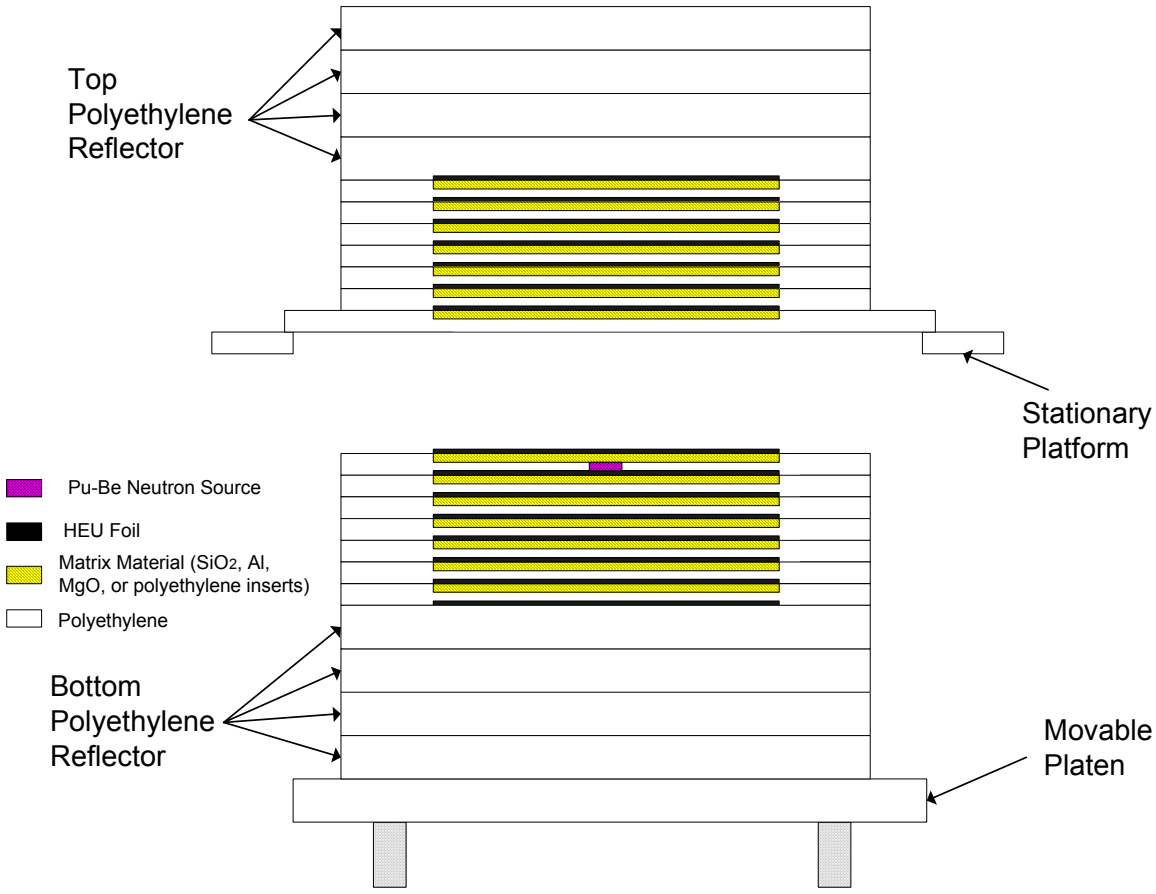

Figure 2. Approximate final configuration for the diluted HEU experiments.

sphere. A 1/M approach to critical was performed following the guidelines of the existing operating procedures.

The starting configuration also contained a Pu-Be neutron source to enhance the neutron multiplication of the system. The neutron leakage from the hand-staking assembly was measured with four BF_3 neutron detectors. The total number of counts in a 100--second time interval was normalized and plotted as unity on a graph of counting rate ratios versus number of unit cells. The next unit was added and the neutron leakage from the assembly was measured. The new total number of counts in a 100--second time interval was divided by the total counts obtained in the previous step. The reciprocal of this number was plotted again on the same graph of counting rate ratios versus number of unit cells. A line that passed through the two points on the graph was extrapolated to the x-axis, which represented the number of unit cells, to obtain the extrapolated critical number of units.

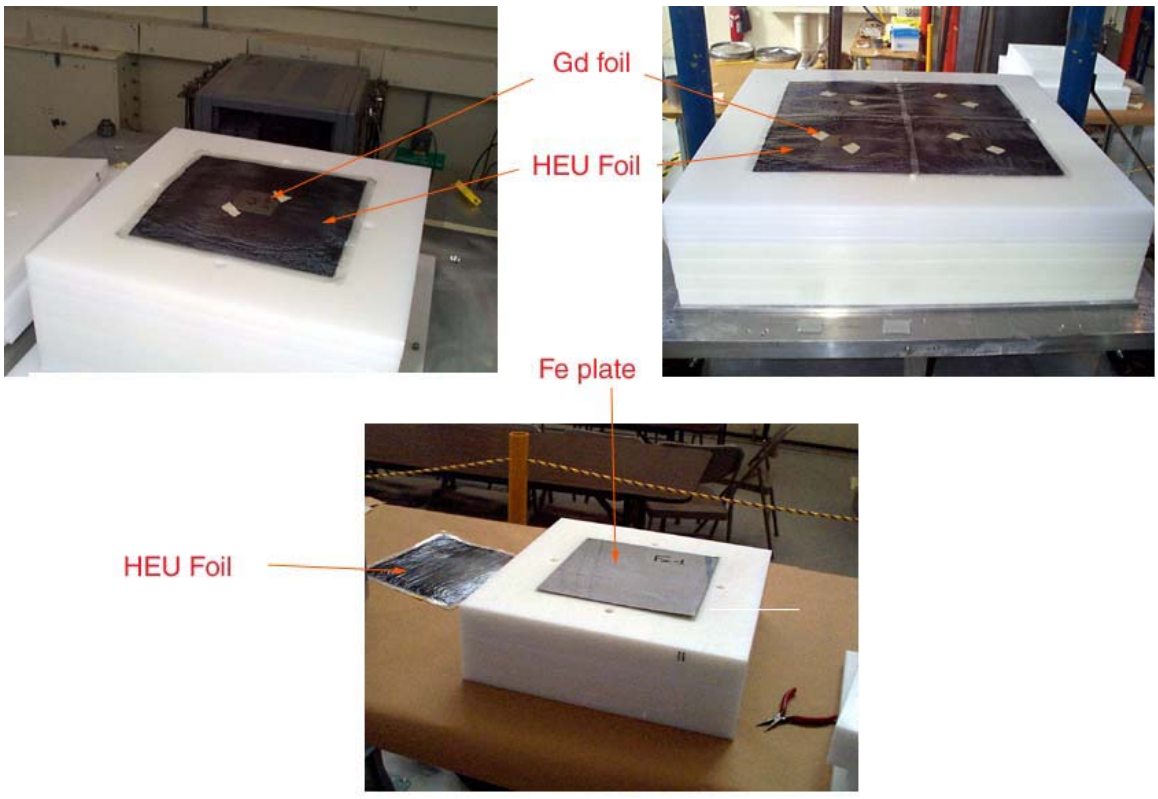

Figure 3. Gadolinium and iron critical--mass experiments.

Once the extrapolated critical number of unit cells was obtained, two guidelines or rules were observed before adding any more fuel into the hand stacking assembly. The first rule was the 75% rule, which simply states that hand-stacking operations should continue until the next step exceeds 75% of the extrapolated critical mass. The second rule was the halfway rule, which states that hand-stacking operations should continue as long as the individual steps taken (addition of fissile material, control rod position, separation distance between two stacks, etc.) do not double the multiplication of the system or the count rate. This rule is based on the assumption that there is a linear relationship between the multiplication of the system and the changing parameter (addition of fuel, gap distance, etc.).

Once the hand-stacking limit was reached, the experiment was split into two parts. The bottom part of the core, which contained approximately half of the critical mass, was placed on the movable platen of the Planet assembly. The top part of the core was placed on a top platform and typically contained two or three unit cells, which represented 5% to 10% of the critical mass. The movable platen, which contained the Pu-Be neutron source, was then raised remotely until it contacted the top portion of the stack. The neutron leakage from the assembly was measured with the same four BF_3 detectors. Because the position of the neutron source changed with respect to the detectors when the stack was split, the total number of counts from the neutron detectors in a 100 second time interval was normalized and plotted as unity on a graph of counting rate ratios versus number of unit cells. After disassembly, uranium foils, diluent materials, and polyethylene plates were added to the top of the stack observing only the halfway rule. The movable platen was raised one more time until both portions of the stack were in direct contact with each other and the neutron leakage was again measured. The total number of counts in a 100--second time interval was divided by the total counts obtained in the previous step and its reciprocal plotted on the same graph to obtain an extrapolated critical number of unit cells. This operation continued until a high multiplication was attained (Fig. 4). For the last units, a 1/M as a function of separation (Fig. 5) was performed to attain the critical separation or the excess reactivity of the system.

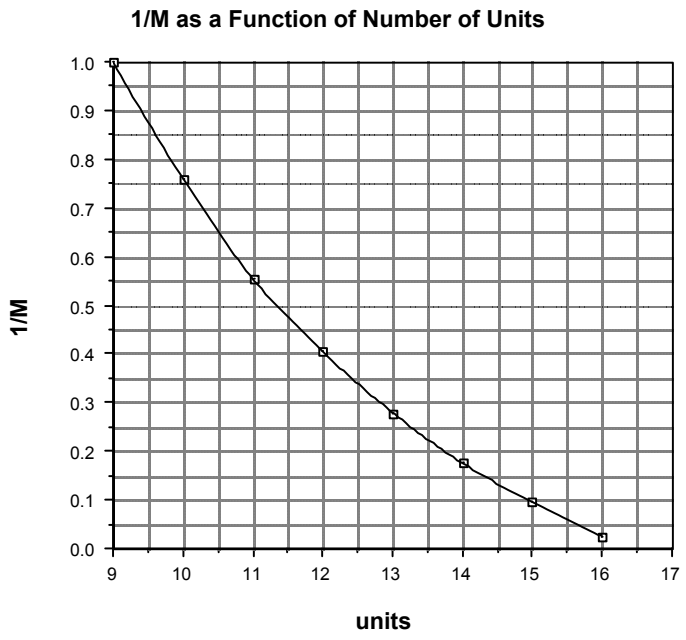

Figure 4. Normalized 1/M as a function of highly enriched HEU foils for ^{235}U-SiO_2-polyethylene experiment. Two HEU foils represent a unit.

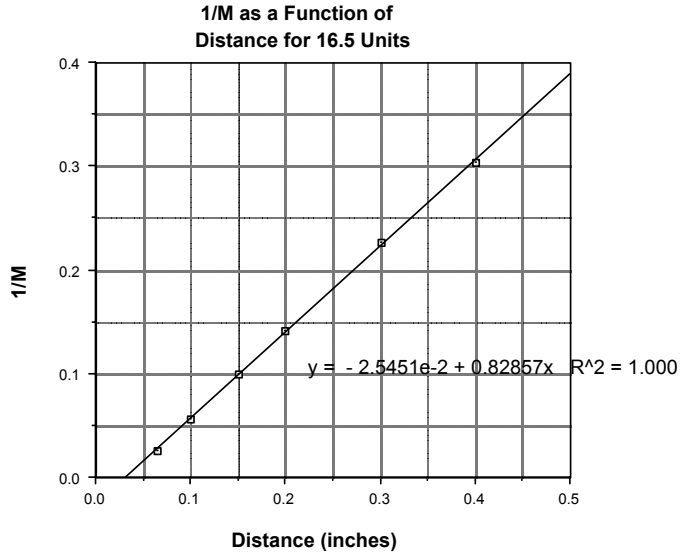

Figure 5. Normalized 1/M as a function of separation for ^{235}U-SiO_2-polyethylene experiment.

4. ROSSI-α MEASUREMENTS

The purpose of the Rossi-α measurements was to establish the reactivity of the system as a function of the separation between the top and bottom part of the core. In addition, the Rossi-α technique[4] correlates time decay constants for the prompt-neutron-linked fission chains with reactivity. These constants represent an eigenvalue characteristic of these particular configurations, which can be calculated by a deterministic or Monte Carlo neutron transport method.

The Rossi-α measurements were performed on two configurations. One of these configurations contained HEU foils diluted with Al plates and polyethylene arranged as shown in Fig. 2. For the other configuration, the Al plates were substituted with SiO_2 and arranged similarly, as illustrated in Fig. 2. One of the polyethylene plates located in the center of the assembly had holes drilled in a radial direction that were used to accommodate highly sensitive ^3He neutron detectors. The data were collected with a time analyzer that had the capability of time tagging each arrival pulse from each of the neutron detectors and sorting them one by one into time bins according to their time of arrival. The stored data could be analyzed using different time widths without having to retake the data. The alphas for both experiments at different subcritical separations were obtained from least square fits to the forms

$$f(t) = A\exp(-\alpha t) + C \quad , \qquad (1)$$

$$f(t) = A\exp(-\alpha_1 t) + B\exp(-\alpha_2 t) + C. \qquad (2)$$

The prompt neutron decay constants at delayed critical were obtained by plotting the alphas at a particular subcritical separation as a function of the inverse count rate and extrapolating linearly to an inverse count rate of zero (delayed critical).

Knowing that α is zero at prompt critical, a linear relationship was established between α and the degree of subcriticality (see Fig. 6). For the $^{235}U/SiO_2$/polyethylene experiment, this relationship is

$$\alpha = (2.231 \pm 0.004)\,(100 - \rho)\ , \qquad (3)$$

where ρ is the reactivity of the system in cents. A similar expression was established for the ^{235}U/Al/polyethylene experiment.

Table II shows the delayed--critical prompt neutron decay constants for ^{235}U/SiO_2/polyethylene, and ^{235}U/Al/polyethylene experiments. It is important to note that for both experiments the least square fit to "one exponential function (Eq. 1)" was not the perfect fit because the systems were operated at high multiplication (high count rate) and the detection system possibly experienced some saturation. Another reason is that the uncorrelated (background) constant, which is represented by C in Eq. 1, increases as the square of the power level and the correlated term (signal), which is the represented by the exponential term, increases proportional to the power. Therefore, the signal to background ratio decreases as the power level increases, which causes the information in the exponential term to be lost and possibly affects the one exponential fit. However, when the neutron source was removed from the system and the measurements were performed for longer periods of time at these high multiplications, the fit approached a "one exponential" function.

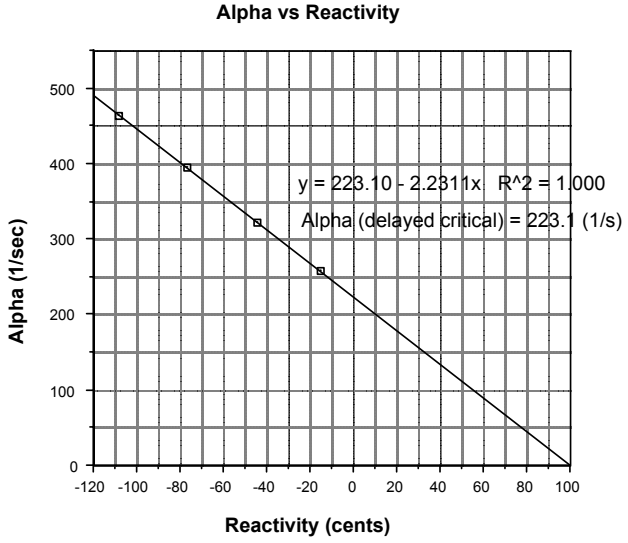

Figure 6. Rossi-α as a function of reactivity for ^{235}U-SiO_2-polyethylene experiment.

In addition, for the two exponential function (Eq. 2), the ratio of the amplitude, A, of the fundamental mode exponential to the second exponential amplitude, B, tends to increase

as the configuration approaches delayed critical. This indicates that the second exponential will tend to diminish as the system approaches the fundamental mode (delayed critical) and that the decay constant, α_1, of the fundamental mode exponential will be similar to the one for the one exponential fit (see Table II).

Table II. Prompt neutron decay constants at delayed critical for uranium diluted with matrix material system.

<table>
<tr><td>Uranium/SiO_2/polyethylene. Si/^{235}U = 21, H/^{235}U = 156. Detector location and source location.</td><td colspan="2">α(1/s) at delayed critical (DC)</td><td>Temperature (°C)</td></tr>
<tr><td rowspan="3">Detectors were placed in the center of the assembly approximately 18.4-cm from the top reflector. Neutron source was placed in the movable platen.</td><td colspan="2">223.1 ± 4.0</td><td rowspan="3">25.5</td></tr>
<tr><td>α_1(1/s) at DC</td><td>α_2(1/s) at DC</td></tr>
<tr><td>218.3 ± 2.0</td><td>13500 ± 3500</td></tr>
<tr><td>Uranium/Al/polyethylene. Al/^{235}U = 60, H/^{235}U = 159. Detector location and source location.</td><td colspan="2">α(1/s) at DC</td><td>Temperature (°C)</td></tr>
<tr><td rowspan="3">Detectors were placed in the center of the assembly approximately 20.3-cm from the top reflector. Neutron source was placed for some runs in the movable part of the core and for other runs in the stationary part of the core.</td><td colspan="2">212.8 ± 9.0</td><td rowspan="3">25.6</td></tr>
<tr><td>α_1(1/s) at DC</td><td>α_2(1/s) at DC</td></tr>
<tr><td>209 ± 9.0</td><td>-</td></tr>
</table>

It is interesting to note that the alphas at delayed critical for both experiments are statistically the same, which indicates that the neutron lifetime is approximately the same for both systems. A calculation was performed with MCNP to determine β_{eff} for both systems. This calculation yielded a β_{eff} of 0.0068 for both experiments. At delayed

critical, $\alpha_{dc} = \beta_{eff}/l$ where l is the prompt neutron lifetime. Thus, the neutron lifetime for both systems is on the order of 30 μs. Finally, the temperature of the experiments was kept within ± 1-°C for each run, which would yield essentially the same alpha if we consider that the reactivity temperature coefficient for these experiments is on the order of $0.003/°C.

5. RESULTS

Table III summarizes the critical configurations obtained as well as the calculated k_{eff} for each system. In some cases, it was deemed appropriate to add a bit more of the extrapolated critical mass to the system to obtain an asymptotic reactor period and in this way to determine the excess reactivity (in cents) above delayed critical through the Inhour equation. An MCNP calculation was performed for each configuration to determine β_{eff} and to be able to convert from reactivity in cents to absolute k.

As seen in Table III, there were two experiments with Gd foils ($Gd/^{235}U$ =0.09, $Gd/^{235}U$ =0.04) that essentially had the same hydrogen content, $H/^{235}U$ =230. These experiments investigated the optimal thickness of the 5.08-cm square Gd foil that would yield the greatest increase in the critical mass. The critical mass changes from 1301 g with no Gd ($H/^{235}U$ =220) to 1893 g with the thin Gd foils to 1958 g with the thicker ones. Based on the results of these experiments, the thicker Gd foils do not make a significant difference in the critical mass when compared with the critical mass obtained with thinner Gd foils. It is interesting to note that the thinner Gd foils may already be 90% black to neutrons and that increasing the thickness is not going to produce a significant increase in the critical mass.

It is important to point out that for $Si/^{235}U$ = 42, and $H/^{235}U$ = 312, the configuration is approaching an infinite cylinder and it may never attain criticality. An MCNP calculation of this experiment including gaps and lamination of the HEU foils yielded a k_{eff} of 0.98. Adding more fuel and moderating materials to the MCNP model caused the k_{eff} to increase and level at 0.99.

Table III. Critical masses and parameters of uranium diluted systems.

Final measured configuration			Critical configuration			keff
Diluent	X/^{235}U, H/^{235}U	Mass of Uranium (g)	Extrapolated critical mass g of U	Core average density (g/cc) U	Core average density (g/cc) diluent	
SiO_2/ polyethylene	Si/^{235}U = 42, H/^{235}U = 312	2196	2878	0.071	For SiO_2 density = 0.74 For CH_2 density = 0.64	-
SiO_2/ polyethylene	Si/^{235}U = 21, H/^{235}U = 156	2233.1	2285.3	0.149	For SiO_2 density = 0.77 For CH_2 density = 0.66	1.002 Exp 1.0070 Cal ± 0.0015 ENDF/B-V[5]
Al/ polyethylene	Al/^{235}U = 60, H/^{235}U = 159	2604	2609.1	0.145	For Al density = 0.93 For CH_2 density = 0.66	1.001 Exp 1.0016 Cal ± 0.0004 ENDF/B-VI[6]
MgO/ Polyethylene	Mg/^{235}U = 18, H/^{235}U = 160	2878	2950.8	0.145	For MgO density = 0.42 For CH_2 density = 0.64	1.0009 Exp 1.0435 Cal ± 0.0004 ENDF/B-VI[7]
Gd/ Polyethylene	Gd/^{235}U = 0.09, H/^{235}U = 230	1951.3	1958.3	0.146	For Gd density = 0.008 For CH_2 density = 0.96	0.9976 Exp 1.00149 Cal ± 0.0005 ENDF/B-VI
Gd/ Polyethylene	Gd/^{235}U = 0.046, H/^{235}U = 228	1811.0	1893.6	0.15	For Gd density = 0.004 For CH_2 density = 0.96	1.0025 Exp 1.00602 Cal ± 0.0005 ENDF/B-VI
Gd/ Polyethylene	Gd/^{235}U = 0.18, H/^{235}U = 245	2801.0	2872.8	0.141	For Gd density = 0.016 For CH_2 density = 0.96	0.9905 Exp 1.00354 Cal ± 0.0005 ENDF/B-VI
Fe/ Polyethylene	Fe/^{235}U = 4.51, H/^{235}U = 224	1388	1408.9	0.154	For Fe density = 0.15 For CH_2 density = 0.96	0.9973 Exp 1.0096 Cal ± 0.0003 ENDF/B-VI[7]
Polyethylene	H/^{235}U = 220	1251.0	1301.4	0.157	For CH_2 density = 0.96	1.0050 Exp 1.0146 Cal ± 0.0005 ENDF/B-VI
Polyethylene	H/^{235}U = 471	1319.0	1331.6	0.073	For CH_2 density = 0.96	0.9969 Exp 0.9909 Cal ± 0.0004 ENDF/B-VI
Polyethylene	H/^{235}U = 239	2233.1	2454.3	0.145	For CH_2 density = 0.96	1.0079 Exp 1.0137 Cal ± 0.0005 ENDF/B-VI

In two cases ($H/^{235}U = 220$, $H/^{235}U = 239$), the bottom part of the core was never in direct contact with the top part of the core because the estimated excess reactivity exceeded \$1.00 (prompt critical) when fully closed. To determine precisely the excess reactivity when the two halves were together, several reactor periods were obtained as a function of separation and converted into reactivity through the Inhour equation. A plot of reactivity as a function of separation was generated, and based on a linear relationship, the excess reactivity was estimated when the system was fully closed. This reactivity in cents was converted to absolute k and the number input into the last column of Table III as the experimental k_{eff}.

For those experiments where the experimental k_{eff} is reported below 1 in table III, the k_{eff} was estimated by the following formula

$$k_{eff} = (M/M_{ec})^{1/3} \quad , \qquad (4)$$

where M is the uranium mass in the experiment and M_{ec} is the extrapolated critical mass from the 1/M plot. This relationship is extremely accurate, especially when the multiplication of the systems is above 100.

The MCNP-4C transport computer code was used to estimate the k_{eff} for each system. For most of the cases, a total of three million histories were run. The code was operated in the k-code mode using continuous energy cross-sections based on ENDF/B-V and VI. The MCNP calculations were performed at room temperature.

For the most part, the calculated values agreed quite well with the experimental k_{eff}. The exception is the experiment that contains MgO. The calculated k_{eff} is approximately 4% higher than the experimental value and it is independent of the type of cross section used. Souto[8] and others are presently investigating this discrepancy and it is believed that the cross-section data currently available for Mg may be the primary source of error observed for this experiment.

6. CONCLUSION

Several experiments were performed at the Los Alamos Critical Experiments Facility to measure the critical mass of higHEUdiluted with matrix materials. For some experiments, Rossi-β measurements were performed to establish a scale of reactivity. These experiments were modeled with MCNP and for the most part the calculated k_{eff} from the code agreed quite well with the experimental values. However, for the MgO experiment, a discrepancy of 4% was found between calculation and experiment. This discrepancy is being investigated.

7. ACKNOWLEDGMENTS

The authors would like to acknowledge Charlene Cappiello and her operating staff for providing the mechanical engineering support needed for the experiments. We thank the operating staff of the Los Alamos Critical Experiments Facility for their help during the operation of the experiments.

8. REFERENCES

1. J. F. Briesmeister, "MCNP-A General Monte Carlo N-Particle Transport Code," Los Alamos National Laboratory report LA-12625-M, Version 4C, (March 2000).
2. D. F. Hollenback, L. M. Petrie, and N. F. Landers, "KENO-IV: A General Quadratic Version of the KENO Program," Oak Ridge National Laboratory report ORNL/NUREG/CDS-2/V2/R6.
3. R. D. O'Dell, F. W. Brinkley, Jr., and D. R. Marr, "User's Manual for ONEDANT: A code Package for One-Dimensional, Diffusion-Accelerated, Neutral-Particle Transport," Los Alamos National Laboratory report LA-9184-M (1982).
4. J. Orndoff, "Prompt Neutron Periods of Metal Critical Assemblies," Nucl. Sci. & Eng., 2, 450, (1957).

5. R. Brewer and R. Sanchez, "HEU-SiO_2-Polyethylene-Reflected Critical Assembly," ANS Transactions, Vol. 84, 282, (2001).
6. D. Loaiza and R. Sanchez, "Benchmark Calculations for the Diluted Highly Enriched (HEU) and Aluminum Experiment," ANS Transactions, Vol. 85, 157, (2001).
7. D. Loaiza, Personal Communications, Los Alamos National Laboratory (May 2002).
8. F. Souto, Personal Communications, Los Alamos National Laboratory (May, 2002).